Turkish Journal of Electrical Engineering & Computer Sciences

http://journals.tubitak.gov.tr/elektrik/

Research Article

Turk J Elec Eng & Comp Sci
(2013) 21: 1260 – 1271

doi:10.3906/elk-1110-7

Analysis of conducted EMI with a standalone solar-powered DC motor

Krishna Kumar CHITTIBABU,[1,*] **Nirmal Kumar ALPHONSE**[2]

[1]Department of Electrical and Electronics Engineering, Periyar Maniammai University, Thanjavur, India
[2]Department of Electrical and Electronics Engineering, INFO Institute of Engineering, Coimbatore, India

Received: 05.10.2011 • **Accepted:** 05.03.2012 • **Published Online:** 12.08.2013 • **Printed:** 06.09.2013

Abstract: The green environment warrants not only researchers, but rather all citizens, to adopt renewable energy sources. One such option is the use of solar energy, especially the conversion of light energy from the sun to electric energy. The conversion of light to electricity with the help of photovoltaic cells (PV), though widely used, has its own problems, such as undesirable electromagnetic interference (EMI), both in radiation and conduction modes. The present research aims to mitigate the unwanted EMI in the conduction mode (to limit the scope of the research). The mitigation of the conducted EMI on a DC/DC buck converter was studied with a standalone 4050 W PV plant. The conducted EMI was measured and the effectiveness of randomization on the spreading of the dominating frequency was examined by a simulation using PSpice software, and the same was validated in real-time measurements. All of the investigations were accomplished using an embedded LPC2129 ARM processor. The theoretical analysis and the experiment results of the conducted noise spectrum were compatible with each other, based on which a randomized duty ratio and a random pulse-position modulation (RPPM) with a fixed carrier frequency scheme were contemplated for adoption.

Key words: Electromagnetic interference, conducted electromagnetic interference, photovoltaic system, pulse width modulation, randomized pulse width modulation

1. Introduction

Electromagnetic interference (EMI), a serious problem in power electronics, takes place during the switching-on and switching-off cycles. The interference is very severe in DC/DC converters and in electrical and electronics equipment. The use of a buck converter is common in the speed control of solar-powered DC motors. The DC motor controlling device creates EMI, which is conducted through the cables to the photovoltaic (PV) cell system, and from there on, it is radiated when the cells act as an antenna [1]. That undesirable radiation interferes with the communication system, as well as any sensitive equipment nearby. The best way to avoid such unwanted and unwarranted interference is to attack the source of the interference, namely the EMI generated by the DC/DC converter switching devices.

The present research paper deals with an attempt to address the conduction-based EMI. The EMI generated during the switching-on and switching-off transitions is transmitted through conduction for low frequencies and via radiation for high frequencies [2]. The conducted EMI could be further classified into common and differential mode noises [3]. The mitigation of EMI could be achieved with or without additional hardware in the circuit [4].

The switching losses and the EMI noise level are controlled by many standards, such as the Federal

*Correspondence: ckk1973@gmail.com

Communication Commission (FCC), International Special Committee and Radio Interference (CISPR), and European Standard (EN) for equipment used in commercial, residential, and industrial applications. Nevertheless, this research adapted the standard EN55022 for the limiting value of the radio frequency emission of the PV system while simulating the model [5].

2. Solar array model

Since experimental analysis with solar cell systems is complicated and cumbersome, an equivalent circuit composed of a current source in parallel with a diode [6] was adopted for simulating the equipment. The current output from the PV cell is directly proportional to the light energy it receives [7]. That relationship was simulated with an equivalent circuit, as shown in Figure 1.

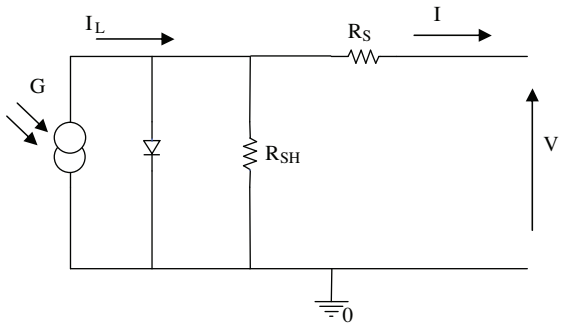

Figure 1. Equivalent circuit of a solar cell.

The I-V relationship for a single cell related to the equivalent circuit is shown below.

$$I = I_L - I_0\{\exp(q(v + IR_S)/nkT) - -1\} - (V + IR_S)/R_{SH} \quad (1)$$

In this model, I_L represents the bipolar current attributed to the light-generated carriers that reach the electrical terminals. The diode represents the PN junction of the solar cell. R_S is the series resistance that accounts for the overall voltage drop and R_{SH} is the shunt leakage resistance [8].

The required simulated outputs were derived by adjusting the diode ideality factor (n) and the resistors R_{SH} and R_S. The simulation was run using PSpice software [9]. By making use of the PSpice software, a theoretical characteristic curve was generated, as shown in Figure 2. With various values for R_S, R_{SH}, and n, experimental results were obtained that are identical to the theoretical characteristic curve validating the same.

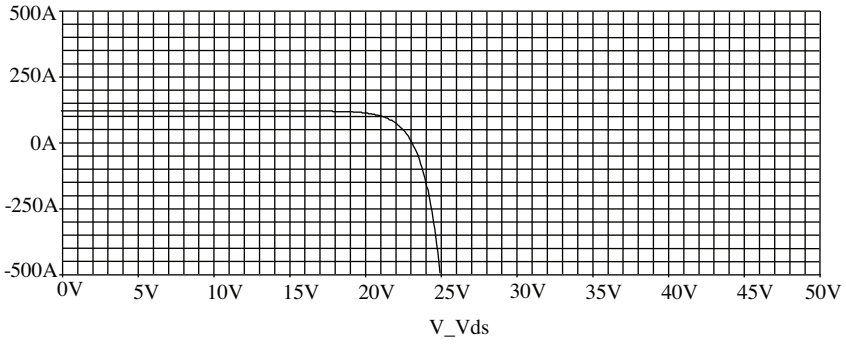

Figure 2. Solar cell VI characteristics.

The data (R_S, R_{SH}, and n) for comparison of the simulated model were taken from the actual values of a working TATA BP solar module (model number: TBP1275M), consisting of 36 cells in series (a commercially available model) [10].

The specifications of the TATA BP model are as tabulated in Table 1. The cells were assumed to be identical, with a limit of 1000 W/m^2, where the maximum voltage is attained at an ambient temperature of 20 °C and a wind speed of 1 m/s.

Table 1. Specifications of the solar module.

S. No.	Parameters	Single module	Existing system
1	Rated power	75 W	4050 W
2	Voltage at maximum power (V_{mp})	17.6 V	35 V
3	Current at maximum power (I_{mp})	4.26 A	115 A
4	Open circuit voltage (V_{oc})	21 V	42 V
5	Short circuit current (I_{sc})	4.6 A	125 A

3. Random switching schemes

Random switching schemes have been used recently to reduce some of the harmonic components of the switching noise generated by the switching devices. The harmonic components around the switching frequency result in EMI and heating effects in the DC motor drive systems [11]. This research attempted the following 5 types of switching schemes for DC/DC converters, to determine the best one.

- Random pulse position modulation (RPPM): delay time (ε_k) changes; frequency (F_k) and duty ratio (d_k) are fixed.
- Random pulse-width modulation (RPWM): d_k changes; F_k and ε_k are fixed.
- Randomized carrier-frequency modulation with fixed duty ratio (RCFMFD): F_k changes; d_k and ε_k are fixed.
- Randomized carrier-frequency with variable duty ratio (RCFMVD): F_k and d_k change; ε_k is fixed.
- Randomized duty ratio and an RPPM with fixed carrier frequency (RDRPPMFCF): d_k and ε_k change; F_k is fixed.

The switching parameters shown in Figure 3, such as the duration of the k*th* cycle (T_k), the duration of the on-state within this cycle (α_k), and the delay from the starting of the switching cycle to the turn-on within the cycle (ε_k), are varied for the 5 different switching schemes [12], according to the characteristics summarized in Table 2.

Table 2. Randomized switching schemes.

Experiment number	Switching schemes	T_k Fixed	α_k	ε_k	$d_k = \alpha_k/T_k$
1	Standard PWM	Fixed	Fixed	Zero	Fixed
2	RPPM	Fixed	Fixed	Randomized	Fixed
3	RPWM	Fixed	Randomized	Fixed	Randomized
4	RCFMFD	Randomized	Randomized	Fixed	Fixed
5	RCFMVD	Randomized	Fixed	Fixed	Randomized
6	RDRPPMFCF	Fixed	Randomized	Randomized	Randomized

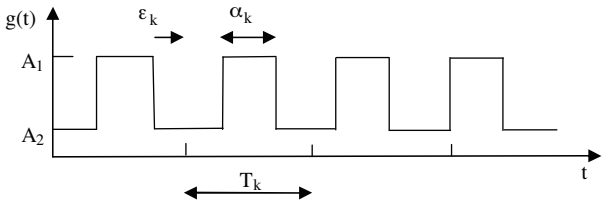

Figure 3. PWM pulses.

4. The experiment setup

This study used a DC motor as the load with a DC/DC converter, which was not used by previous researchers. Most previous studies were carried out with resistive or inductive loads rather than a solar-powered DC motor load, which is the defending parameter in the present research.

The research was carried out on a 4050 Wp PV plant, installed on a roof at Periyar Maniammai University in Thanjavur, Tamil Nadu, India. This plant was installed by the university students and provides energy for utilities, including the lighting load and heating load of the hostel.

The PV plant consists of 54 solar modules and is divided into 6 rows of 9 modules each. The modules in each row are connected in parallel, and each row is connected in series. The existing PV plant is modified as 2 modules in series (2×17.6 V $= 35$ V) and 27 modules in parallel (27×4.26 A $= 115$ A). For the modified system, the real time voltage measured at maximum power (V_{mpp}) is 24 V, the current at maximum power (I_{mpp}) is 105 A, the open circuit voltage (V_{oc}) is 42 V, and the short circuit current (I_{sc}) is 125 A. Figure 4 shows a photograph of the PV plant.

For the DC motor, an input voltage of 24 V, a maximum current of 5 A, and a maximum rpm of 3000 were used for this investigation. The hardware setup and the circuit arrangement of a chopper-fed DC motor are shown in Figures 5 and 6, respectively. The chopper switch used is a fast-power metal-oxide semiconductor field-effect transistor (MOSFET), with a high switching frequency and a low drain-to-source resistance that produces a high EMI. The test setup follows the CISPR 16 standard. The conducted EMI was measured with a military standard MIL-STD462-D line impedance stabilization network (LISN) in the frequency range of 150 kHz to 30 MHz. To provide standard impedance for the measurement, the available EMCO make, model no: 3810/2 with 50 Ω, 50/250 Hz, and 9 kHz to 30 MHz LISN, was used. The spectrum analyzer used was the HAMEG model HM5012/5014, with 150 kHz to 1.5 GHz.

Figure 4. Solar panels.

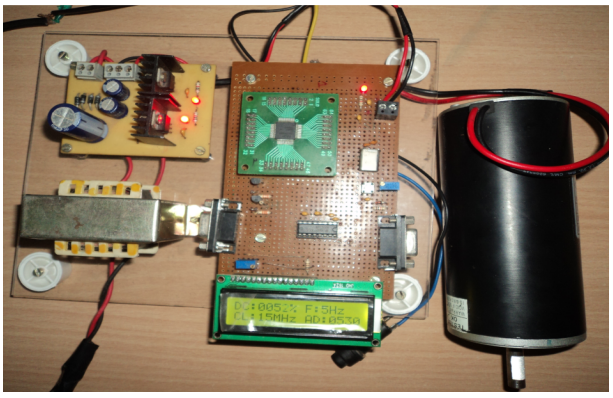

Figure 5. Hardware setup.

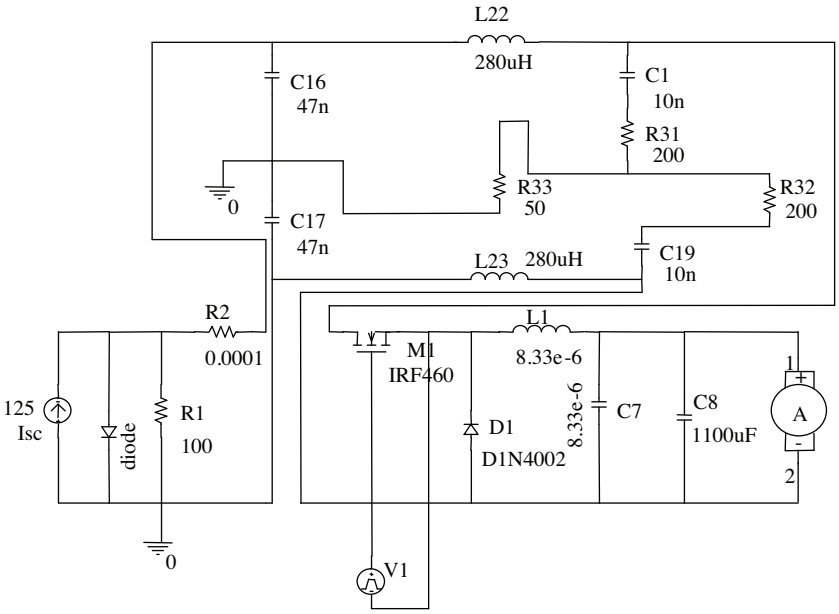

Figure 6. Circuit for simulation.

5. Experiment on the standard PWM technique

Standards like CISPR and FCC rules part 15 have set emission frequency limits of 150 kHz to 30 MHz. Hence, in this paper, a bandwidth range of 150 kHz to 30 MHz was considered for analysis. Figure 7 shows the simulated results of the conducted EMI when a standard PWM technique for the duty cycle of 0.8 was used. The experiment was carried out by considering the delay time ε_k as 0 and T_k as 0.8 ms. The measurement revealed significant conducted noise that was generated within the DC motor and the converter module. It can be observed from Figure 7 that in the bandwidth range of 150 kHz to 1 MHz, the peak values of the noise exceed a 60 dBμV limit. In the frequency range of 1 MHz to 30 MHz, the peak values reached up to 75 dBμV. In accordance with standard EN55022, the quasi-peak limit varied from 65 dBμV to 55 dBμV for the bandwidth range of 150 kHz to 600 kHz; for the bandwidth range of 600 kHz to 5 MHz, the quasi-peak limit was 55 dBμV; and for the 5 MHz to 30 MHz frequency range, it was 60 dBμV. It was observed that the resonant peaks in the range of 150 kHz to 1 MHz exceeded the quasi-peak limit range insisted on by the generic emission standard EN55022 by 9 dBμV. For the high frequency bandwidth range of 1 MHz to 30 MHz, it was found that the peak values were more than the prescribed limit, and they exceed it by 20 dBμV.

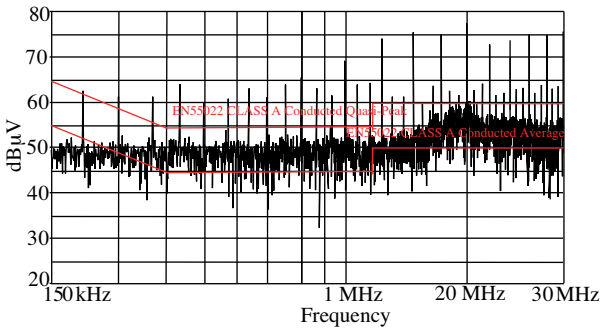

Figure 7. Conducted noise spectrum for a standard PWM.

Figure 8 shows the experimental results of the conducted noise when a standard PWM technique was applied to the MOSFET-based buck converter. It was observed that in the bandwidth range of 150 kHz to 1 MHz, the peak values of the conducted noise exceeded 70 dBμV. In the frequency range of 1 MHz to 30 MHz, the peak values reached more than 80 dBμV. The simulation results were compared with real-time measurements and it was found that there was a variation of 8 dBμV in the bandwidth range of 150 kHz to 30 MHz.

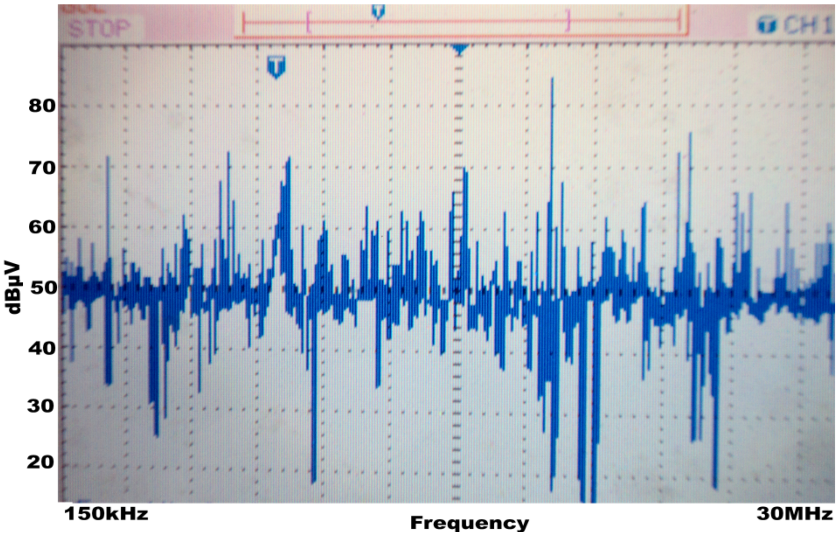

Figure 8. Measured conducted noise spectrum for a standard PWM.

6. Experiment on the RPWM technique

Figure 9 shows the simulated results of the conducted EMI when the RPWM technique was used. For the RPWM scheme, α_k and d_k varied randomly and the maximum value of ε_k was fixed as 0.12 ms. The experiment was carried out by considering the randomness level of the on-time (α_k) from 70% to 80% of the T_k (0.8 ms). It was observed that in the frequency range of 150 kHz to 600 kHz, the resonant peaks are less than 50 dBμV. The peak level of the conducted noise was maintained as approximately 50 dBμV in the bandwidth range of 150 kHz to 10 MHZ. In the high-frequency range of 10 MHz to 30 MHz, 5 peaks were observed, out of which 1 peak had a value of 65 dBμV, whereas the rest of the peaks had values in the range of 56 to 60 dBμV. The average value of the conducted noise spectrum for the RPWM technique was 48 dBμV, which was 3 dBμV higher than

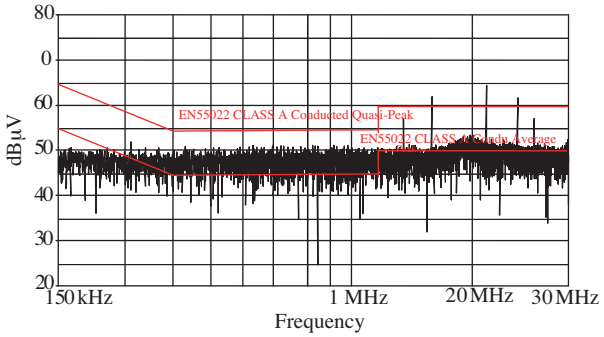

Figure 9. Conducted noise spectrum for a RPWM.

the average value prescribed by the standard EN55022. Figure 10 shows the real-time experimental results. It was observed that within the bandwidth range of 150 kHz to 1 MHz, the peaks were within 50 dBμV, and the number of peaks above 60 dBμV was found to be increased in the bandwidth range of 1–30 MHz.

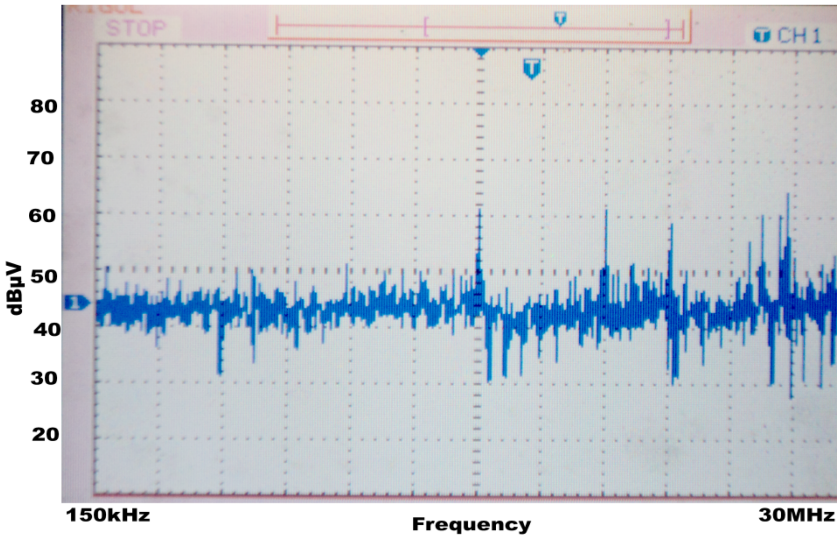

Figure 10. Measured conducted noise spectrum for a RPWM.

7. Experiment on RPPM technique

Figure 11 shows the simulated results of the conducted EMI when the RPPM technique for the duty cycle of 0.8 was used. For the RPPM scheme, the ε_k varied randomly and the maximum values were limited to the value of (α_k – T_k), and the other parameters, such as F_k, α_k, and d_k, were fixed. The experiments were carried out by considering the randomness level of the delay time ε_k from 15% to 25% of the T_k (0.8 ms). It was observed that at the frequency range of 150 kHz to 1 MHz, the resonant peaks were within 45 dBμV to 55 dBμV. In the high frequency range of 1 MHz to 30 MHz, the peaks of the conducted noise were in the range of 45 dBμV to 66 dBμV. A maximum peak value of 66 dBμV was observed at around the 20 MHz range. The peaks observed in the frequency range of 150 kHz to 1 MHz did not exceed the quasi-peak limit of 65 dBμV of the standard EN55022. In the high frequency range of 1 MHz to 30 MHz, the peaks exceeded the quasi-peak limits by approximately 7 dBμV.

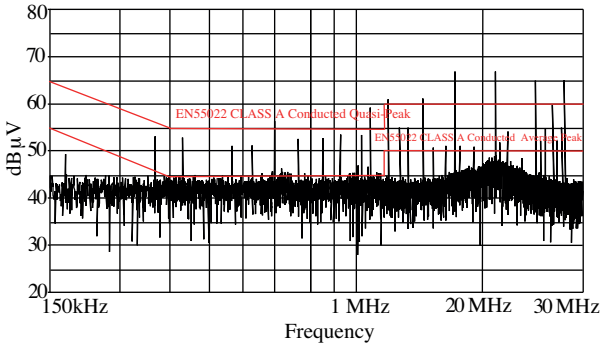

Figure 11. Conducted noise spectrum for a RPPM.

In Figure 12, it can be observed that the number of resonant peaks was increased in the bandwidth range of 150 kHz to 1 MHz, and it was more than the limit range of the standard EN55022. In the high frequency range of 1 MHz to 30 MHz, the resonant peaks had the same number when compared with the simulation results.

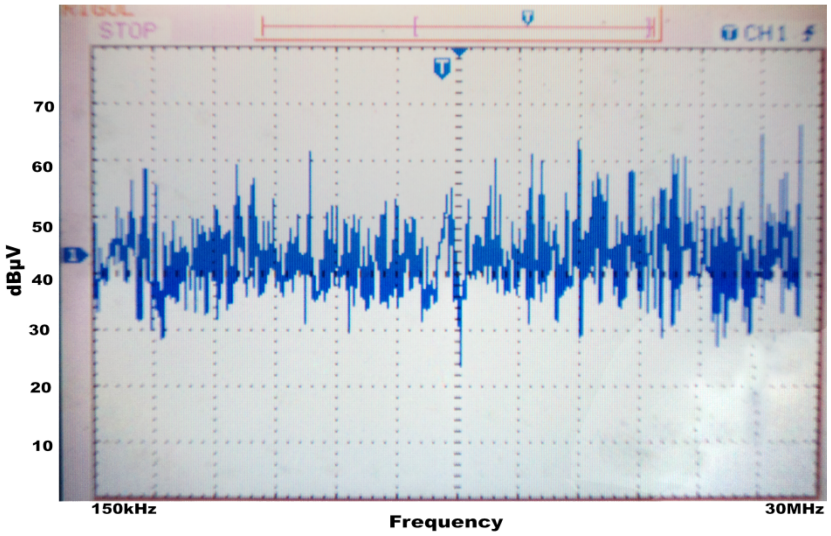

Figure 12. Measured conducted noise spectrum for a RPPM.

8. Experiment on RCFMFD technique

In this technique, the parameters F_k, T_k, and α_k were randomized. The time period was randomized by $\pm 12.5\%$ of 0.8 ms. α_k was varied by maintaining the 70% time limit of T_k. Figure 13 shows the simulated results of the conducted EMI when the RCFMFD technique was used for the duty cycle of 0.8. In the frequency range of 150 kHz to 600 kHz, there was only 1 peak that reached the 50 dBμV limit, and the noise level was also less than the average value of the conducted noise specified by the standard EN55022. In Figure 13, it can be observed that resonant peaks existed within the range of 150 kHz to 1 MHz, but they were lower than the quasi-peak limit. In the high-frequency range of 1 MHz to 30 MHz, the maximum peaks were within the allowable limit of 60 dBμV; however, 2 peaks exceeded the quasi-peak limit of 60 dBμV by around 20 MHz.

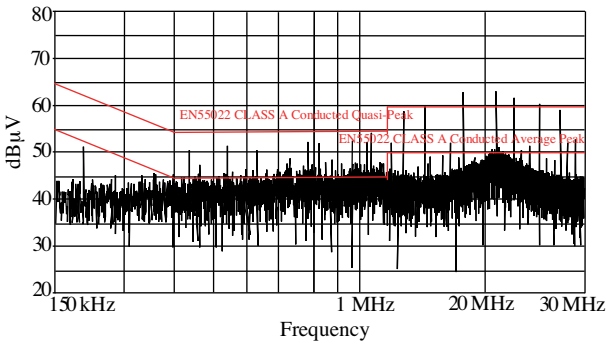

Figure 13. Conducted noise spectrum for a RCFMFD.

In Figure 14, it can be observed that the resonant peaks in the bandwidth range of 150 kHz to 1 MHz exceeded the conducted average limits by 10 dBμV. In the frequency range of 1 MHz to 30 MHz, 3 peaks

exceeded the allowable limit of 60 dBμV.

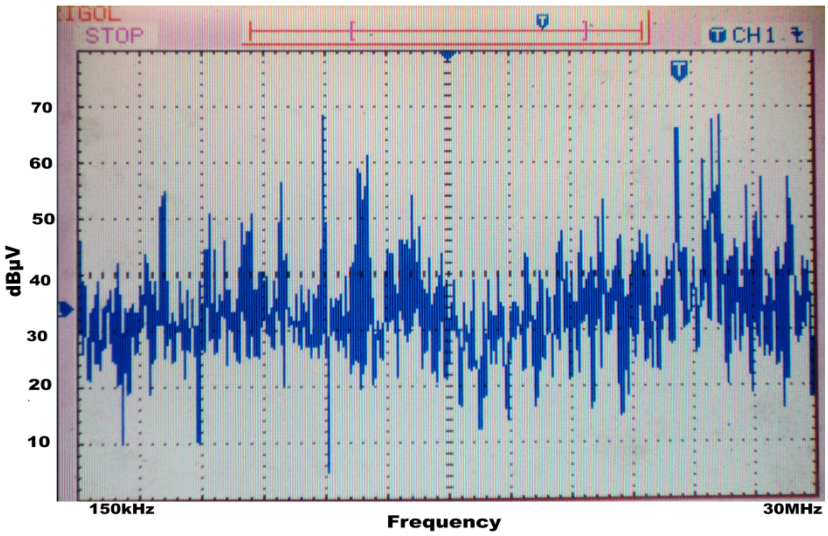

Figure 14. Measured conducted noise spectrum for a RCFMFD.

9. Experiment on RCFMVD technique

This technique was implemented by varying F_k, T_k, d_k, and α_k in a randomized manner while ε_k was kept constant. The time period was randomized by $\pm 12.5\%$ of 0.8 ms. The experiment was carried out by considering the randomness level of the on-time (α_k) from 70% to 75% of the T_k. Figure 15 shows the simulated results of the conducted EMI when the RCFMVD technique was implemented. It was observed that the conducted noise was within the quasi-peak limits in the frequency range of 150 kHz to 1 MHz. However, in the high-frequency range of 1 MHz to 30 MHz, the resonant peaks were at a level of 65 dBμV, exceeding the limit specified by 5 dBμV.

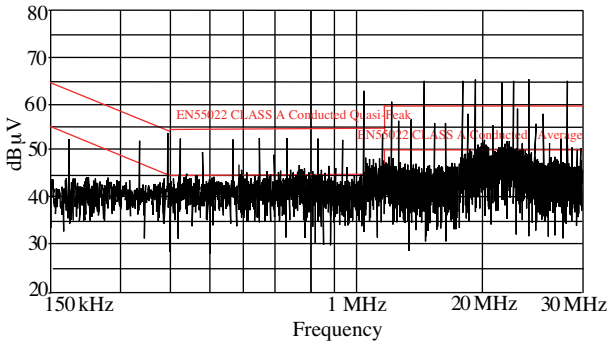

Figure 15. Conducted noise spectrum for a RCFMVD.

Figure 16 shows the conducted noise spectrum when the RCFMVD scheme was implemented. It was observed that the number of resonant peaks was increased in the frequency range of 150 kHz to 1 MHz and it exceeded the quasi-peak limits of the EN55022. In the high-frequency range of 1 MHz to 30 MHz, the resonant peaks reached approximately 68 dBμV.

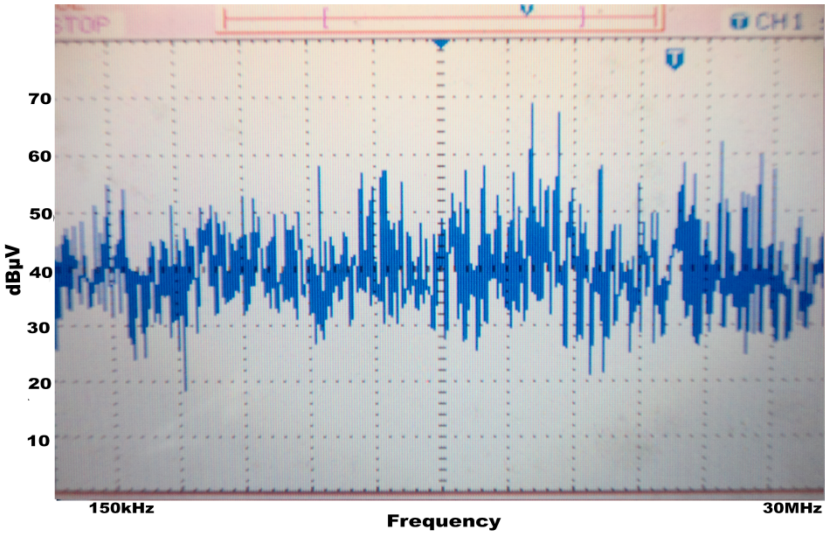

Figure 16. Measured conducted noise spectrum for a RCFMVD.

10. Experiment on the RDRPPMFCF technique

The experiment with the RDRPPMFCF was carried out by randomizing the parameters d_k, ε_k, and α_k, and by keeping F_k and T_k as constants for the PWM control of the DC/DC converter. Figure 17 shows the conducted noise spectrum of the RDRPPMFCF modulation technique. From the graph, it can be observed that the average conducted noise value of the spectrum was around 42 dBμV and that the noise peaks were less than 50 dBμV in both the low- and high-frequency ranges. It was verified that the noise level was less than the quasi-peak level and that the average value of the noise spectrum was below the level specified by the standard.

In Figure 18, it can be observed that the experimental results were below the average and quasi-peak limits specified by the EN55022.

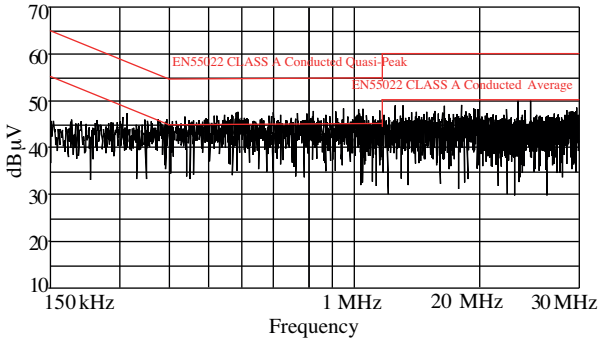

Figure 17. Conducted noise spectrum for a RDRPPMFCF.

11. Comparative study

Various randomized modulation schemes under the PWM technique were adopted for experiments to mitigate the EMI, restricting the spectrum between 150 kHz to 30 MHz. The results obtained were tabulated as shown in Table 3. It was segmented in to 3 bands.

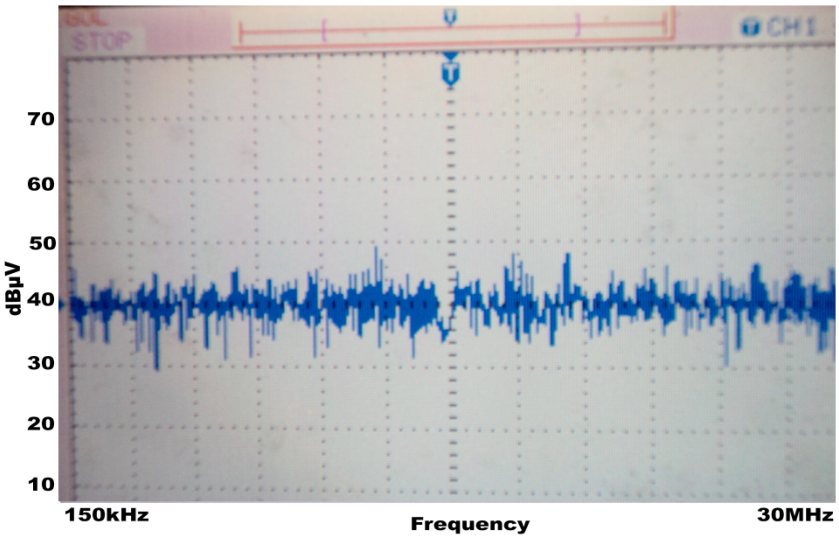

Figure 18. Measured conducted noise spectrum for a RDRPPMFCF.

Table 3. Measured conducted noise.

PWM schemes	150 kHz to 600 kHz Quasi-peak limit: 65 to 55 dBμV	600 kHz to 1 MHz Quasi-peak limit: 55 dBμV	1 MHz to 30 MHz Quasi-peak limit: 60 dBμV
Ordinary PWM	Exceeded by 9 dBμV	Exceeded by 9 dBμV	Exceeded by 15 dBμV
RPWM	Attenuated by 5 dBμV	Attenuated by 5 dBμV	Exceeded by 5 dBμV
RPPM	Attenuated by 2 dBμV	Attenuated by 1 dBμV	Exceeded by 7 dBμV
RCFMFD	Attenuated by 10 dBμV	Attenuated by 3 dBμV	Exceeded by 4 dBμV
RCFMVD	Attenuated by 7 dBμV	Attenuated by 2 dBμV	Exceeded by 5 dBμV
RDRPPMFCF	Attenuated by 20 dBμV	Attenuated by 8 dBμV	Attenuated by 12 dBμV

11.1. Analysis

It was observed that the quasi-peak value exceeded beyond the limits set by the standard throughout the spectrum range (150 kHz to 30 MHz). Hence, an alternate was looked for in the mitigation of the EMI. Although the RPWM, RPPM, RCFMFD, and RCFMVD schemes resulted in attenuation in the spectrum between 150 kHz to 1 MHz, they were not successful in attenuating beyond 1 MHz.

The quasi-peak value beyond 1 MHz was higher than the set value specified; hence, although the 4 schemes were better than the previous scheme, they were not recommended.

The scheme under the RDRPPMFCF provided fairly good attenuation throughout the spectrum range of 150 kHz to 30 MHz; hence, it was recommended for mitigating the EMI.

12. Conclusion

From the experimental results, to mitigate the conducted EMI on a DC/DC buck converter with a low-power standalone PV system connected to a DC motor, it could be safely recommended that the RDRPPMFCF be used for mitigating the EMI, since the results obtained meet the EN specifications. Hence, the present research advocates the adaption of the same for reducing the effect of conducted EMI.

References

[1] H. Häberlin, "New DC-LISN for EMC-measurements on the DC side of PV systems realisation and first measurements at inverters", European Photovoltaic Solar Energy Conference, 2001.

[2] C. Krishnakumar, A. Nirmalkumar, B. Karthikeyan, R. Abinaya, "Impact of variable switching frequency over power loss on converter topologies", International Journal of Computer Applications , Vol. 8, pp. 6–11, 2010.

[3] K. Wada, T. Shimizu, "Reduction methods of conducted EMI noise on parallel operation for AC module inverters", IEEE 38th Annual Power Electronics Specialist Conference, pp. 3016–3021, 2007.

[4] A. Farhadi, A. Jalilian, "Modeling and simulation of electromagnetic conducted emission due to power electronics converters", IEEE International Conference on Power Electronics Drives and Energy Systems, pp. 1–6, 2006.

[5] D. Hamza, P. Jain, "Conducted EMI in grid-tied PV system", IEEE Telecommunications and Energy Conference, pp. 1–7, 2010.

[6] L. Castaner, S. Silvestre, Modelling Photovoltaic Systems Using PSpice, New York, Wiley, 2002.

[7] T. Ikegami, T. Maezono, F. Nakanishi, Y. Yamagata, K. Ebihara, "Estimation of equivalent circuit parameters of PV module and its application to optimal operation of PV system", Journal of Solar Energy Materials and Solar Cells, Vol. 67, pp. 389–395, 2001.

[8] D.D. Nguyen, B. Lehman, "Modeling and simulation of solar PV arrays under changing illumination conditions", IEEE Workshop on Computers in Power Electronics, pp. 295–299, 2006.

[9] A. Aziz, K. Kassmi, A. Mortinez, F. Olivie, "Symbolization of the electric diagram of the marketed solar panels in the Orcad-Pspice environment", Moroccan Journal of Condensed Matter, Vol. 7, pp. 38–41, 2006.

[10] R. Ramaprabha, B.L. Mathur, "Impact of partial shading on solar PV module containing series connected cells", International Journal of Recent Trends in Engineering, Vol. 2, pp. 56–60, 2009.

[11] F. Mihalic, D. Kos, "Conductive EMI reduction in DC-DC converters by using the randomized PWM", IEEE International Symposium on Industrial Electronics, Vol. 2, pp. 809–814, 2005.

[12] G.M. Dousoky, M. Shoyama, T. Ninomiya, "FPGA based spread spectrum schemes for conducted noise mitigation in DC-DC power converters: design, implementation, and experimental investigation", IEEE Transactions on Industrial Electronics, Vol. 58, pp. 429–435, 2011.